Fouling mechanisms of dairy streams during membrane distillation

Angela Hausmann[a,b], Peter Sanciolo[a], Todor Vasiljevic[b], Mike Weeks[c], Karin Schroën[d], Stephen Gray[a] and Mikel Duke[a*]

[a]Institute for Sustainability and Innovation, College of Engineering and Science, Victoria University, PO Box 14428, Melbourne, Victoria, 8001, Australia

[b]Food Systems Research Unit, College of Health and Biomedicine, Victoria University, PO Box 14428, Melbourne, Victoria, 8001, Australia

[c]Dairy Innovation Australia Ltd, Werribee, Victoria, 3030, Australia

[d]Department of Agrotechnology and Food Sciences, Wageningen University, Wageningen, The Netherlands

*: mikel.duke@vu.edu.au

Abstract

This study reports on fouling mechanisms of skim milk and whey during membrane distillation (MD) using polytetrafluoroethylene (PTFE) membranes. Structural and elemental changes along the fouling layer from the anchor point at the membrane to the top surface of the fouling layer have been investigated using synchrotron IR micro-spectroscopy and electron microscopy with associated energy dispersive X-ray spectroscopy (EDS). Initial adhesion of single components on a membrane representing a PTFE surface was observed *in-situ* utilizing reflectometry. Whey components were found to penetrate into the membrane matrix while skim milk fouling remained on top of the membrane. Whey proteins had weaker attractive interaction with the membrane and adhesion depended more on the presence of phosphorus near the membrane surface and throughout to establish the fouling layer. This work has given detailed insight into the fouling mechanisms of MD membranes in major dairy streams, essential for maintaining membrane distillation operational for acceptable times, therewith allowing further development of this emerging technology.

1.0 Introduction

Membrane distillation (MD) is a thermally driven membrane process and relies on a highly hydrophobic porous membrane to maintain a liquid-vapour interface. Common membrane materials for MD are polypropylene (PP), polyvinylidene fluoride (PVDF) and PTFE [1, 2]. The highest performing membrane material for MD is PTFE due to its high hydrophobicity, chemical inertness and open porous structure [3]. Fouling in the MD process is different to that observed in pressure driven processes such as RO. The low operating pressure used in MD may potentially lead to a less compact, more easily removed, fouling layer. Also, since only volatile compounds pass through the membrane pores, the potential for in-pore fouling is minimized in MD applications. Studies of MD processes have, however, revealed that penetration of foulants into the membrane can occur in some instances [4]. There is a need for a better understanding how dairy components interact with MD membranes and accumulate at the membrane surface. This understanding may allow better control of performance of membrane distillation via better mitigation of fouling.

The high hydrophobicity of MD membranes can result in the establishment of hydrophobic interactions between the membrane and any solutes that have hydrophobic components, such as proteins and fats. While hydrophilic coatings may be a possible avenue to reduce the fouling that results from these hydrophobic interactions [5-7], simple uncoated membranes have advantages in terms of lower cost and can be easier to manage over time as there is no requirement to maintain a specialised surface coating.

There are numerous studies on fouling phenomena occurring with dairy components [8-13], however little can be found on the actual mechanisms behind the fouling. Most studies focus on membrane performance, not investigating kinetics behind fouling phenomena observed. In cases where fouling layer compositions have been studied, analyses focus on the average composition of the surface deposits or visualizing the top surface deposits, but not on the underlying deposit layers. For those studies that did investigate cross-sections of fouling layers [10, 14], no elemental or

structural analysis has been conducted leading to an incomplete understanding of the deposition kinetics of dairy foulants. In particular, dairy fouling studies on hydrophobic membranes as used for MD are almost non-existent.

This work not only describes fouling phenomena observed during MD but also identifies the underlying chemistry considering the kinetics of the fouling layer buildup, with a focus on the initial adhesion reactions and fouling compositional profiles. Such exploration and understanding of fouling mechanisms is critical to successfully introduce MD systems to dairy operations, and in particular for the development of effective cleaning and antifouling strategies.

2.0 Materials and Methods

2.1 Direct contact membrane distillation (DCMD) system

The equipment used to test DCMD with dairy solutions is shown in Figure 1. PTFE flat-sheet membranes (Ningbo Chanqi, China) of 0.5 µm nominal pore size and about 20 µm thickness, with a woven (scrim) polypropylene support were used in a laboratory scale Osmonics SEPA CF module (GE Osmonics, Minneapolis, MN, USA) housing providing an effective membrane area of 0.014 m^2. A peristaltic pump with two heads provided a steady flow on both, feed and permeate, sides. On the permeate side, cold stripping water was circulated to provide the temperature difference and to allow vapour condensation on the cold side. All four inlet and outlet temperatures were measured as well as both inlet pressures. Flux was measured by continuously and automatically recording permeate weight gain in the closed circuit.

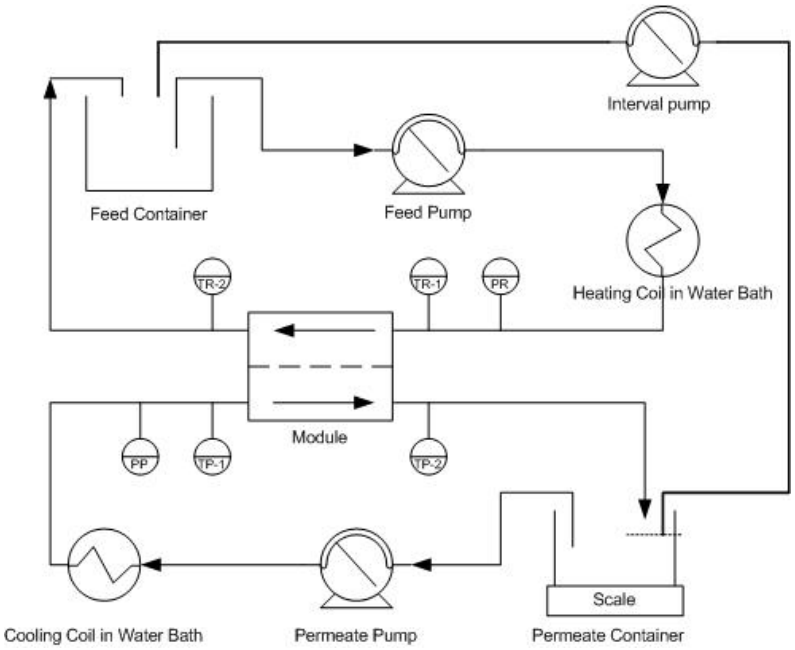

Figure 1: Laboratory scale DCMD set-up for operation at constant concentration

A new membrane was used for each experiment and performance was benchmarked under standardized conditions: 54 °C feed in, 5 °C permeate in, flow of 0.047 $m \cdot s^{-1}$ (200 mL/min) on both sides of the membrane. The feed temperature was limited to 54 °C in order to avoid effects of protein denaturation as whey proteins start to unfold at temperatures higher than 60 °C [15]. A relatively low flow rate was chosen to ensure the feed pressure never exceeded 10 kPa to exclude any effect from an increasing pressure. Moderate increases in pressure have been shown to compress PTFE MD membranes [16] that led to reduced flux, but it was not expected to be significant in these experiments because the pressure was never observed to go beyond 10 kPa. Deionised water was used for benchmarking and flux recorded after a one hour stabilization phase. Operating conditions for experiments were kept consistent with benchmarking parameters.

As hydrophobic membrane distillation membranes are very sensitive to fat [17, 18], the dairy systems tested in this paper were very low in fat: <0.1 % for skim milk and whey. Reconstituted powder dispersions were prepared from commercial samples obtained from a local supplier and composition shown in Table 1. These preparations were tested at 20 % total solids dispersed in

deionised water. To prevent microbial growth, 0.2 $g \cdot L^{-1}$ of sodium azide (Sigma-Aldrich, St Louis, USA) was added to the feed solution. Every test was carried out for an extended period of time (~20 hours) which is a targeted runtime in the dairy industry where daily cleaning is necessary due to microbial growth.

Table 1: Compositions of powders used in this study, supplier information (all in %)

Powder	Moisture	Fat	Protein	Lactose	Ash	Ca	K	Na	P
Skim milk	3.5	1.0	35.0	50.5	7.8	1.29	2.02	0.43	1.01
Whey	5.0	1.0	11.5	73.5	9.7	0.52	2.03	0.86	

2.2 Wet-chemistry analyses of fouling layers

To analyse the composition of fouling layers after experiments, the membranes were cut into 14 cm^2 strips and soaked in 2 ml of deionised water over night at 50 °C. The membrane surface was then scraped with a surgical blade to remove all matter remaining on the membrane into the original soaking water. The resulting solution was left at 50 °C again until all particulates were dissolved. After this removal procedure there was no visible fouling left on the membrane and no visible particles in the soaking water. The concentration of foulant compounds per cm^2 of membrane was calculated from the concentration in the soaking water determined by the difference in the initial and final weight.

2.2.1 Lactose HPLC

Lactose in the fouling layer samples was detected by a HPLC system (Shimadzu, Kyoto, Japan) as reported elsewhere [19]. For this, 900 µl samples were filtered through 0.45 µm syringe filter into HPLC sample bottles. An Agilent Zorbax Carbohydrate column and a light-scattering detector were used. The flow rate was set to 1.4 ml per minute, the mobile phase consisted of 75 % acetonitrile and 25 % HPLC grade water. Standards of 0.05, 0.1, 0.2, 0.5, 1 and 2% lactose were run to produce a calibration curve. The injection volume was 10 µl.

2.2.2 Inductively Coupled Plasma Atomic Emission Spectroscopy (ICP-AES)

Fouling layer samples were analysed for selected cations (K^+, Na^+, Ca^{2+}, Mg^{2+}, P) using a Shimadzu ICP E-9000 unit (Kyoto, Japan). Samples containing a high amount of proteins were subjected to a wet-digestion step prior to ICP-analysis as suggested by Kira et al. [20]. Aliquots of 100 µL of sample were mixed with 1 mL of HNO_3 (65 % v/v) and heated to boiling temperature for at least an hour or until de-coloration occurred leaving a clear solution as evidence of organics being fully digested. The digested sample and 10 mL of HNO_3 (5%) were transferred into a volumetric flask and filled to the standard volume using deionised water to dilute samples as needed to achieve a total solids concentration below 0.1 %. Samples not containing organics were acidified using the same amount of HNO_3 but were not subjected to a digestion step. All samples were filtered through a 0.45 µm syringe filter into ICP sample bottles. All calibration solutions were prepared using standard solutions for each element following a dilution scheme to establish a calibration curve for each mineral.

2.2.3 Total Organic Carbon (TOC) and Total Nitrogen Analysis (TN)

Samples were analysed for total organic carbon and total nitrogen using a Total Organic Carbon and Total Nitrogen Analyzer (Shimadzu V_{CSH}). Sample preparation only involved dilution to below 100ppm of carbon. For total nitrogen analysis samples needed to be diluted below 50 ppm of nitrogen. Standard solutions of 100 ppm potassium hydrogen phthalate (KHP) for TOC and 50 ppm potassium nitrate (KNO_3) for TN analysis were used to confirm the original calibration. To convert the nitrogen reading to milk protein, the nitrogen measurement was multiplied by a Kjeldahl factor of *6.38* [21]. This is equivalent to the Kjeldahl method which is officially recognised as a standard reference method in food science and technology [22].

2.3 Fouling layer cross section analysis

2.3.1 Scanning Electron Microscopy (SEM), coupled with Energy Dispersion Spectrometry (EDS)

The morphology of the fouling layers after MD testing was studied using a bench-top SEM (Nikon/JEOL Neo- Scope JCM-5000, Melville, NY) applying a voltage of 10 kV and using a secondary electron detector. Study of the changes in elemental composition along the fouling layers from the anchor point at the membrane to the top of the fouling layer was performed using a SEM coupled with energy dispersion spectrometry (EDS). This analysis was carried out from the surface by observing inside the cracks of the fouling layer which occurred as a result of the drying step. This conveniently excluded artifacts due to sample preparation. Samples were dried in a vacuum oven over night and 2 min gold coated for conventional SEM and platinum coated for SEM-EDS analysis. Cross-sections were prepared by a cryo-snap method [23]. The membrane pores were hydrated using ethanol, then ethanol was replaced by water and the membrane strip placed into a flint glass test tube which was then submerged in liquid nitrogen for 5 minutes before freeze snapping the glass tube with the fully hydrated membrane inside. The cleaved membranes still embedded in ice were then dried as described earlier. Embedding the membrane in a continuous matrix of water/ice during fracturing reduces artifacts.

2.3.2 Reflectometry

Reflectometery is an optical measurement for component adhesion on even surfaces. The principle and detailed method of this technique are explained in detail elsewhere [24, 25]. Strips of prime grade 150 mm silicon wafers type P/B with <1−0−0> orientation (WaferNet Inc., San Jose, CA, USA) were cleaned with ethanol, dried and spin-coated (30 seconds, 2500 rpm) with an amorphous fluoropolymer (DuPont Teflon AF). To ensure full vaporisation of volatiles from the Teflon solution coating, silicon strips were heated to 350 °C for at least one hour. The Teflon coating represents the

membrane material and uniform thickness of the coating was checked by computer controlled null ellipsometry (Sentech instruments Gmbh). The coated silicon strips were then inserted into the measurement cell of the reflectometer. Buffer and fouling solutions entered the cell directly onto the Teflon surface via gravity feeding and were removed by overflowing from the cell. All experiments were carried out at flow rates between 0.8 and 1.2 $mL \cdot min^{-1}$. Fouling solutions need to be of low concentration for this analysis due to the laser passing through the solution. They were prepared by dissolving 1 $g \cdot l^{-1}$ of the respective foulant in a phosphate buffer at pH 7 to reproduce conditions of the natural dairy streams.

A linearly polarized He/Ne laser beam entered the measurement cell through a 45˚ glass prism and left the cell through a second 45˚ prism. It was split into its parallel and perpendicular components by a polarizing beam splitter, intensities of the normal and parallel components were recorded over time. The intensity change of the reflected polarized laser was converted to adsorbed amounts using a 5-layer matrix model [26, 27]. This model requires the thickness of the polymer layer and refractive indices of the various layers, as determined by ellipsometry (see above). For the silicon substrate, a refractive index of 3.85 with imaginary part 0.02 was used [25] and the refractive index used for the PTFE top layer was 1.35. A refractive index increment (dn/dc) of 0.187 was used for whey proteins and 0.207 for caseins [28, 29].

2.3.3 Synchrotron Infrared microscopy

Infrared spectroscopy at the Australian Synchrotron was used to map organic sub-layers of the fouling layer. To allow for examination in transmission mode, samples were cut thin enough for the beam to pass through the sample. This was done at Hawthorn Histology, Melbourne, by embedding the fouled membranes in paraffin, microtoming to 10 µm thick sections and subsequent fusing of the thin sections on CaF_2 windows (Crystran Ltd, UK) at 60°C to enable effective transmission analysis of the membrane and fouling layers.

3.0 Results and Discussion

3.1 Fouling development over time

Fouling reversibility during periodic switching from skim milk to water during MD treatment is shown in Figure 2. Flux decline during skim milk treatment occurred rapidly (within minutes) and flux recoveries were only partial within 30 minutes of processing with water. Even after long recovery periods (i.e. hours) in pure water, flux only returned to about 50% of the original pure water value.

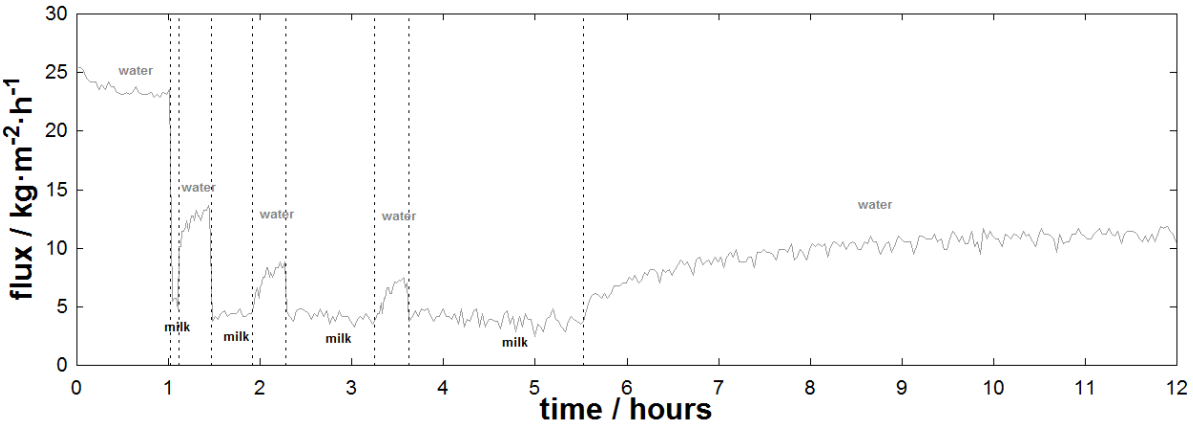

Figure 2: Flux during MD of skim milk. Water is introduced for 20 minutes after 5 min, 30 min, 1 hour and 2 hours running to show flux recovery; Long term recovery at the end of the experiment to identify maximum achievable flux recovery

The fouling reversibility for a whey solution is shown in Figure 3. In contrast to the flux observed during skim milk processing, switching back to water after a short fouling period restored water flux to its original stable value of around 22 $kg \cdot m^{-2} \cdot h^{-1}$. Extended fouling periods led to a continuously dropping flux (Figure 3b), however upon extended water operation flux returned closely (within 10 %) of its original stabilised water value.

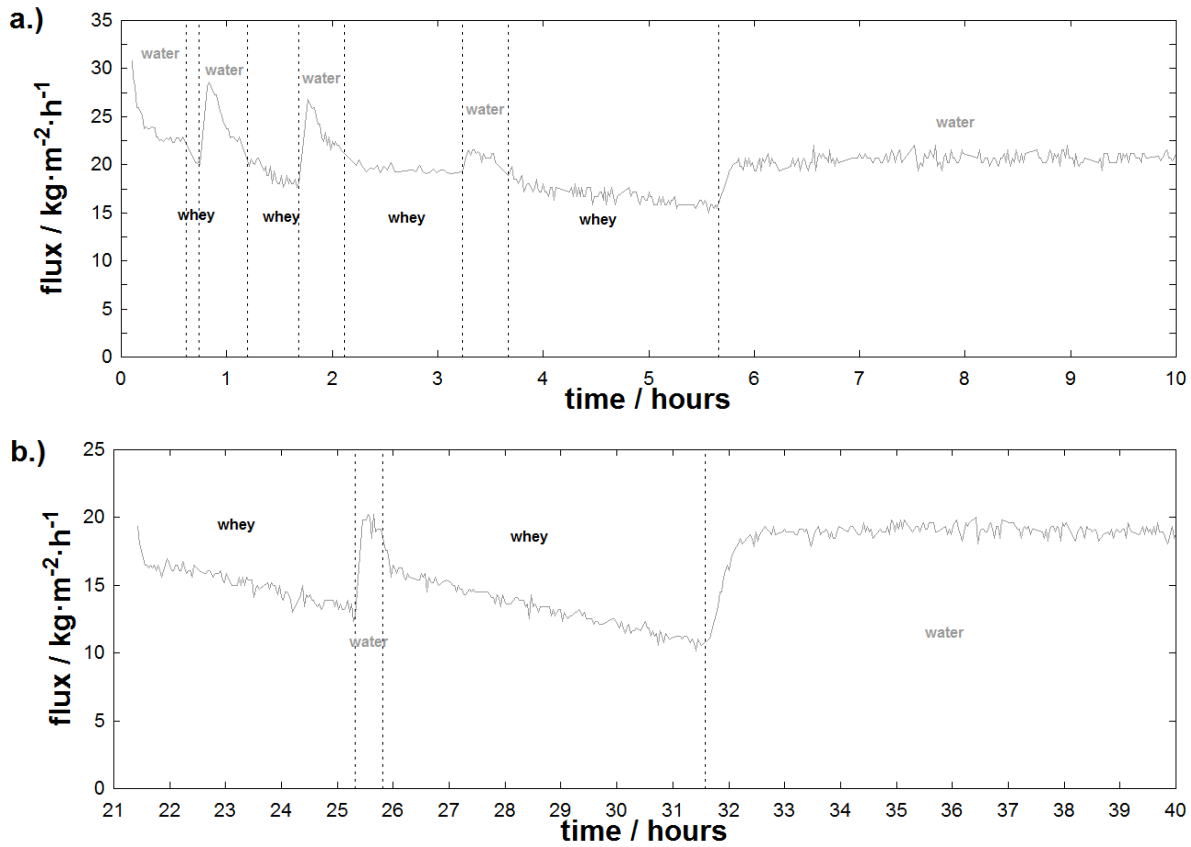

Figure 3: Flux during MD of whey. Water introduced for a.) 20 minutes after 5 min, 30 min, 1 hour and 2 hours b.) 4 and 6 hours running to show original flux return; long recovery at the end.

An interesting difference between the flux profiles of skim milk and whey is the flux trends that take place during the first few water permeation stages. In the skim milk experiment, water permeation results in an increase in flux towards the clean water flux after skim milk permeation stages at the beginning of the experiment. In the whey experiment, however, water permeation initially results in a flux close to the initial level of clean water at the start of the experiment, and this then decreases to a slightly lower level. These changes are difficult to explain, but may involve a temporary increase in effective surface area (i.e. air/water interface) resulting from the restoration of hydrophobicity of the membrane as the foulant is removed during water permeation, and the subsequent decrease in contact angle at the PTFE surface as the foulant is dissolved and decreases the surface tension of the water. A decrease in surface tension of the solution has been found to decrease the contact angle on the PTFE surface [30].

The effect of time on the formation of the skim milk and whey fouling layers is shown in the SEM images in Figure 4. The fouling layer of skim milk was relatively constant between 5 and 30 minutes of operation and covered the entire membrane area. The layer then continued to grow in thickness but reached a steady state after 1 hour. Flux with the skim milk solution on the other hand, did not drop much between 5min and 2 hours of operation (Figure 2). This indicates that the thin layer formed after 5min was equally permeable as the layer formed after 2 hours. The rate limiting factor appears to be the limited surface area exposed to water due to the low porosity of the fouling layer or also reduced vapour pressure due to the higher solids content of the fouling layer. Extended build up of the fouling layer seems to lead to increased resistance for water transport to the surface, but this seems to be small compared to the limitation of the evaporation area. Whey fouling on the other hand started with patches on the membrane that developed to a layer that covered the entire membrane surface after 6 hours of operation. The fouling layer grew in terms of surface area covered, whereas skim milk fouling layer was more homogenous from the beginning and developed in thickness, and this can also explain the observed differences in flux reduction (rate).

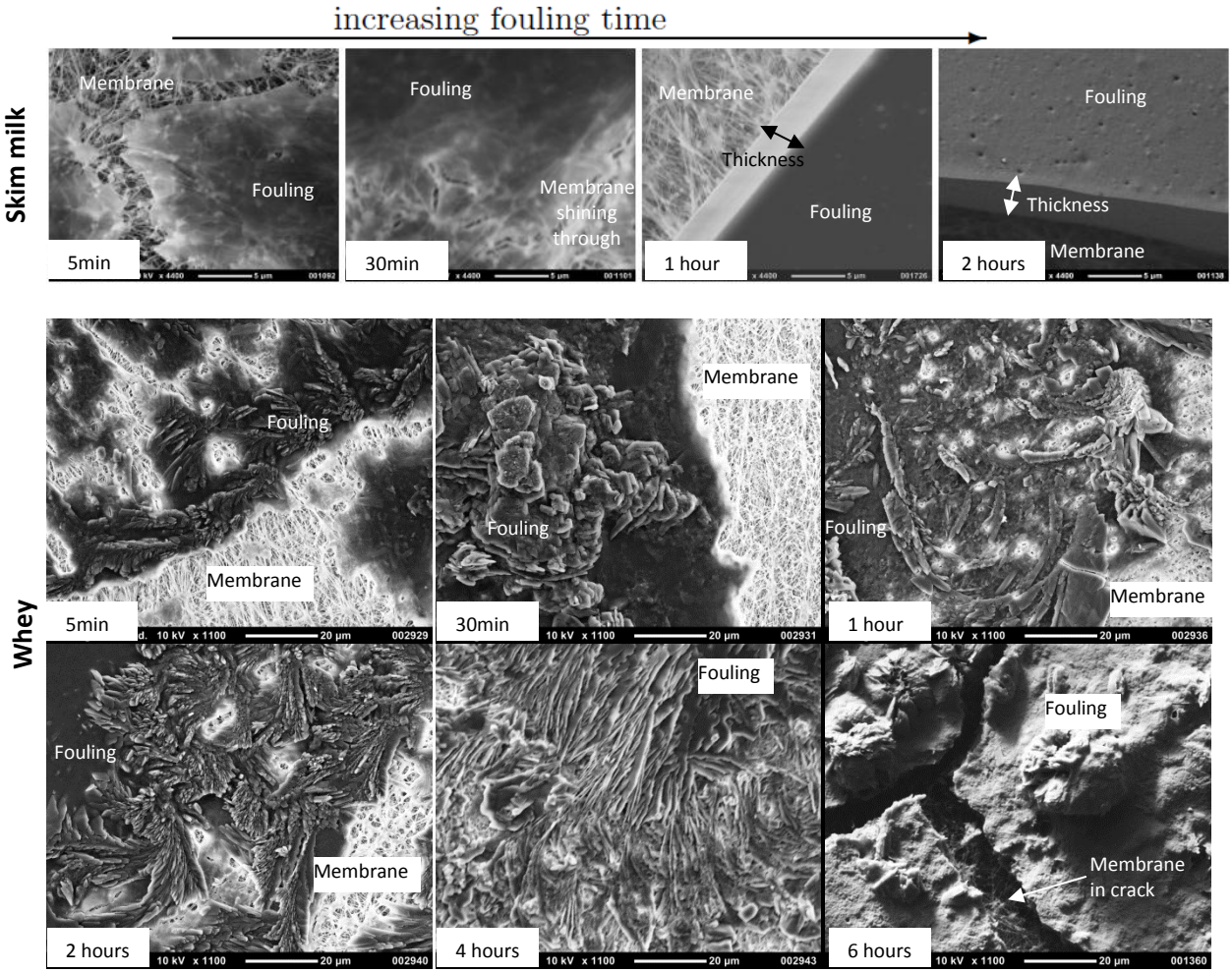

Figure 4: SEM of skim milk fouled membranes (top) from left to right: 5 min fouling, 0.5 hour, 1 hour, 2 hours and whey fouled membranes (bottom): 5 min fouling, 0.5 hour, 1 hour, 2 hours, 4 and 6 hours

Changes in composition of the collected fouling layer for skim milk and whey fouled membranes over time are shown in Figure 5. Skim milk fouling appears to have occurred in different stages. First, caseins and salts deposited on the membrane surface, while lactose was only detected after longer fouling times. Protein deposition was higher for skim milk at all fouling stages, however protein content of the fouling layer increased substantially after 30 min of fouling, whereas whey fouled membranes showed a gradual rise in protein concentration initially with a great accumulation between 2 and 4 hours. Also, the ratio between the three major components did not change as

substantially during whey fouling. Salts were found to deposit faster than lactose which is consistent with the skim milk samples.

Overall, whey flux decline appeared to follow the growth of fouling layer thickness and increased deposited amount of solids, flux is therefore controlled by diffusion resistance in this layer. However for skim milk, the total deposited amount does not correlate with the observed differences in flux. Compared to whey, the fouling layer was thinner but flux was much lower, especially in the first few minutes. As described above, we could explain this difference due to either a denser fouling layer or also reduced vapour pressure associated with the concentrated solids. Since the skim milk fouling layer grew continuously over 2 hours (Figure 4 and Figure 5) and the increase in thickness had an insignificant effect on flux (Figure 2), it suggests that diffusion resistance did not govern the flux decline as it was for whey. Water vapour pressure reduction due to dried material at the membrane surface is not linked to the thickness of fouled substance so it is possible that dry fouling substance influenced the flux independently to thickness. Uncovering the separate properties of vapour pressure of fouling layers and linking this to membrane performance is subject of our ongoing work in this area.

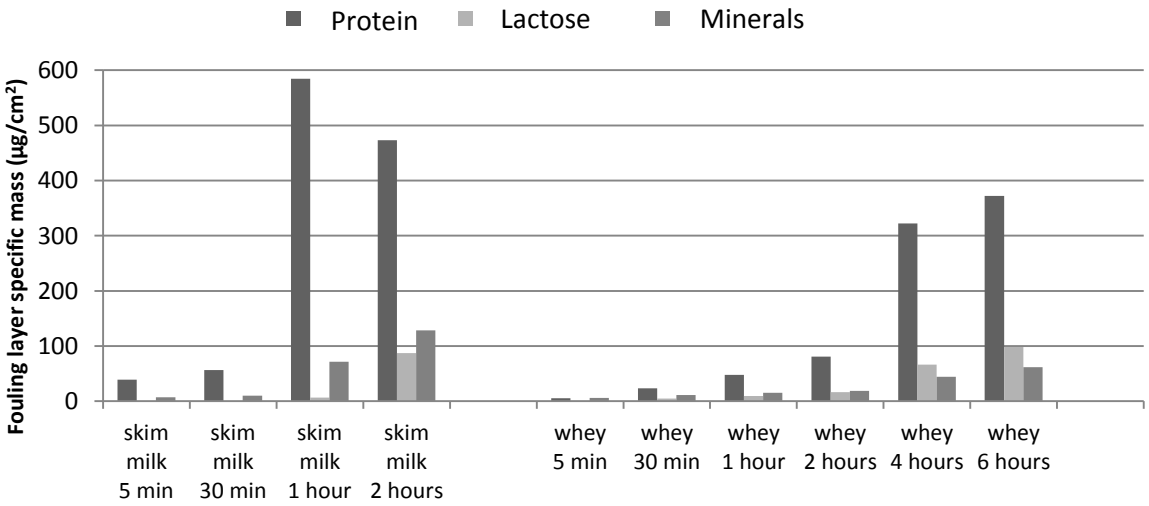

Figure 5: Changes in composition of fouling layer developing over time

During fouling development of whey, the amount of protein and salt at very early stages was almost equal. This was followed with greater amounts of protein accumulation in the fouling layer while the salt concentration increased only slightly. Table 2 shows the mineral composition of the fouling layers with time. The key minerals involved in deposition were calcium and phosphorus, however they appeared to play a more significant role in skim milk fouling than in whey fouling. For skim milk, the high calcium and phosphorus content can be explained by the nature of caseins in skim milk. These proteins are present in form of micelles, which contain colloidal calcium phosphate via calcium ion bounding to phosphoserine residues of these proteins [31]. For the whey, the considerable calcium and phosphorus content of the fouling layer suggests that protein adsorption involves calcium and phosphate interaction with the protein and/or with the membrane. The negative charge of PTFE can lead to charge interaction with salts [32]. Once a layer of proteins had formed, the whey proteins could interact with each other via salt bridging with few salts adsorbed onto the membrane surface. Generally, whey proteins are known to aggregate at a high concentration - a condition which occurs near the membrane and is further influenced by temperature and pH [33].

Table 2: Mineral content of fouling layers developing over time

	Concentration [all in µg/cm^2]				
Sample Name	**Ca**	**K**	**Mg**	**Na**	**P**
Skim milk – 5 min	7	1	0	2	1
Skim milk – 30 min	6	1	0	0	1
Skim milk – 1 hour	39	5	3	7	17
Skim milk – 2 hours	74	8	3	5	41
Whey – 5 min	4	1	0	0	0
Whey – 30 min	4	2	0	4	0
Whey – 1 hour	6	2	1	4	0
Whey – 2 hours	13	3	0	2	1
Whey – 4 hours	20	12	1	5	5
Whey – 6 hours	32	13	1	5	6

3.2 Initial adhesion

Proteins are known to adsorb on hydrophobic surfaces due to their hydrophobic or amphoteric character [34-36]. As shown in Figure 5, the fouling layer largely consisted of proteins. The extent and rate of adsorption appeared to be governed by the nature and type of dairy proteins and the presence of calcium phosphate. An insight into adsorption behaviour of the individual dairy proteins and their combinations onto the PTFE surface was gained via the use of reflectometry.

To further elucidate complex protein fouling mechanisms of milk, the rate and extent of adsorption of the three casein groups present in milk is shown in Figure 6: α-, including both α_{s1} and α_{s2} casein, β- and κ-casein, individually and in pairs. All three caseins exhibited different adsorption behaviour. K-Casein was found to adsorb faster than the other caseins, while α_s-casein was found to absorb the slowest and to the least extent. β-Casein was also slow to adsorb, but it adsorbed to a greater extent than the other two caseins. Combining two casein groups greatly accelerated overall deposition and resulted in fastest adsorption rates when combined with κ-casein. The final adsorbed amount was in between that of the respective single caseins. When all three caseins were combined, however, the rate and extent of adsorption was less than for the paired combinations. This is consistent with the formation of a more stable mixed casein micelle when the three caseins are present, which does not

adsorb as readily. Micelles in milk suspensions are stabilized by the presence of k-casein on the surface of the micelle where it functions as an interface between the hydrophobic casein micelle interior and the aqueous environment [37].

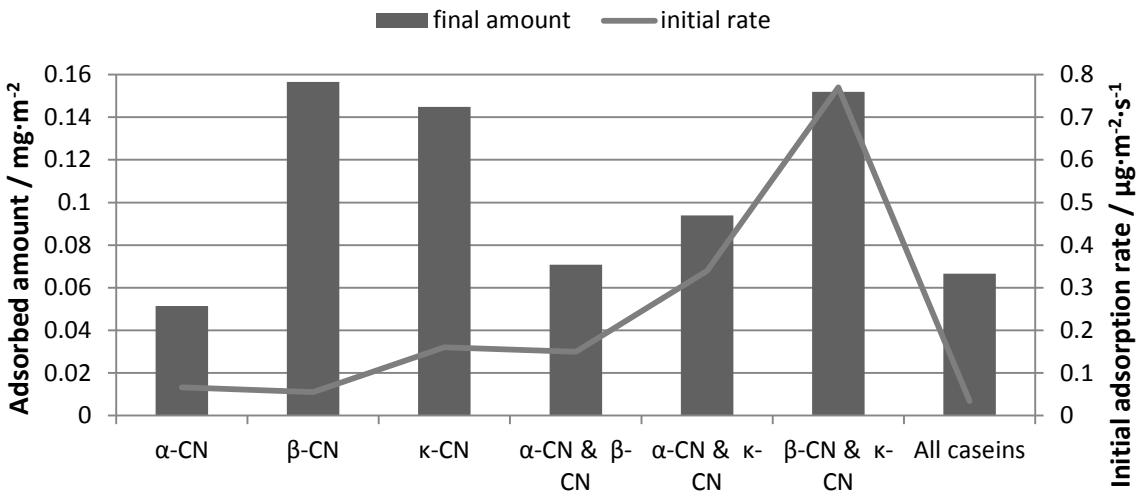

Figure 6: Adsorbed amount and adsorption rate of caseins on a PTFE coating. CN = casein

Whey proteins as shown in Figure 7 adsorbed more slowly and resulted in lower adsorbed amounts compared to single caseins. Bovine serum albumin (BSA) led to lowest adsorbed amount, α-lactalbumin (α-La) was the slowest to adsorb to the PTFE surface, whereas β-lactoglobulin (β-Lg) showed the fastest and highest adsorption amongst the single proteins. It has been previously shown that β-Lg contributes more to membrane fouling than α-La due to the ability of β-Lg to form protein sheets on the membrane surface [38]. All combinations of two whey proteins reached slightly higher total adsorbed amounts than individual whey proteins. Also, the combination of α-La and BSA accelerated deposition, and was faster than respective single proteins. The total deposition amount was only slightly increased when all whey proteins were combined together compared to the combination of α-La and β-Lg, but the adsorption rate was much faster. In contrast to the situation with caseins where the combination of all the caseins appeared to lead to the formation of a more stable mixed micelle which does not adsorb as readily, the combination of the different whey

proteins seem to decrease the stability of the protein solution, thereby increasing adsorption rate and extent.

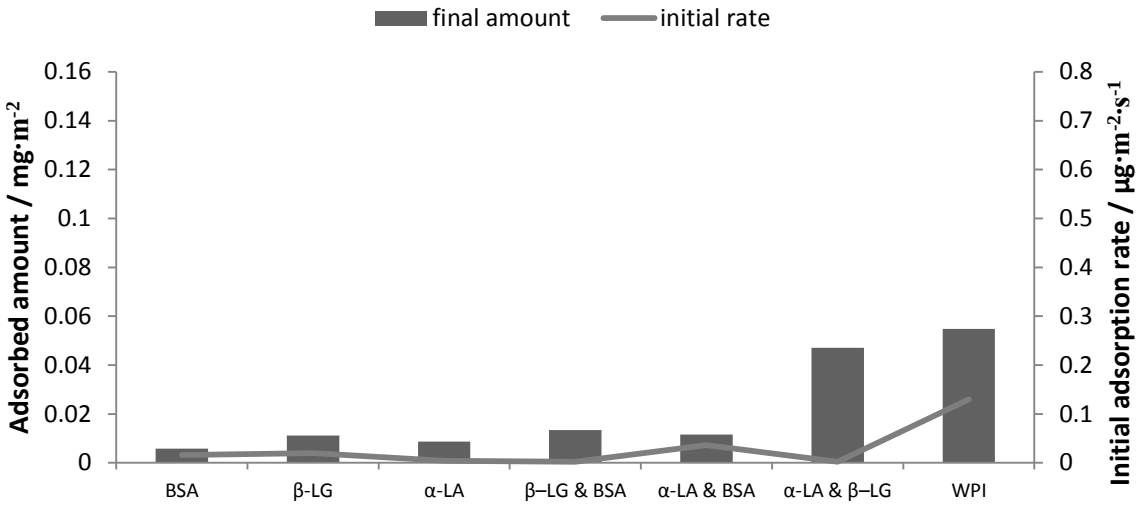

Figure 7: Adsorbed amount (bars) and adsorption rate (line) of whey proteins on a PTFE coated surface determined by reflectometry. BSA = Bovine serum albumin, β-LB = beta-lactoglobulin, α-LA = alpha-lactalbumin, WPI = whey protein isolate

3.3 Fouling layer cross section analysis

3.3.1 SEM imaging

SEM pictures of the membranes cross-sections are shown in Figure 8 with a new PTFE membrane on the left, a skim milk fouled membrane including the fouling layer in the middle and a whey fouled membrane on the right hand side.

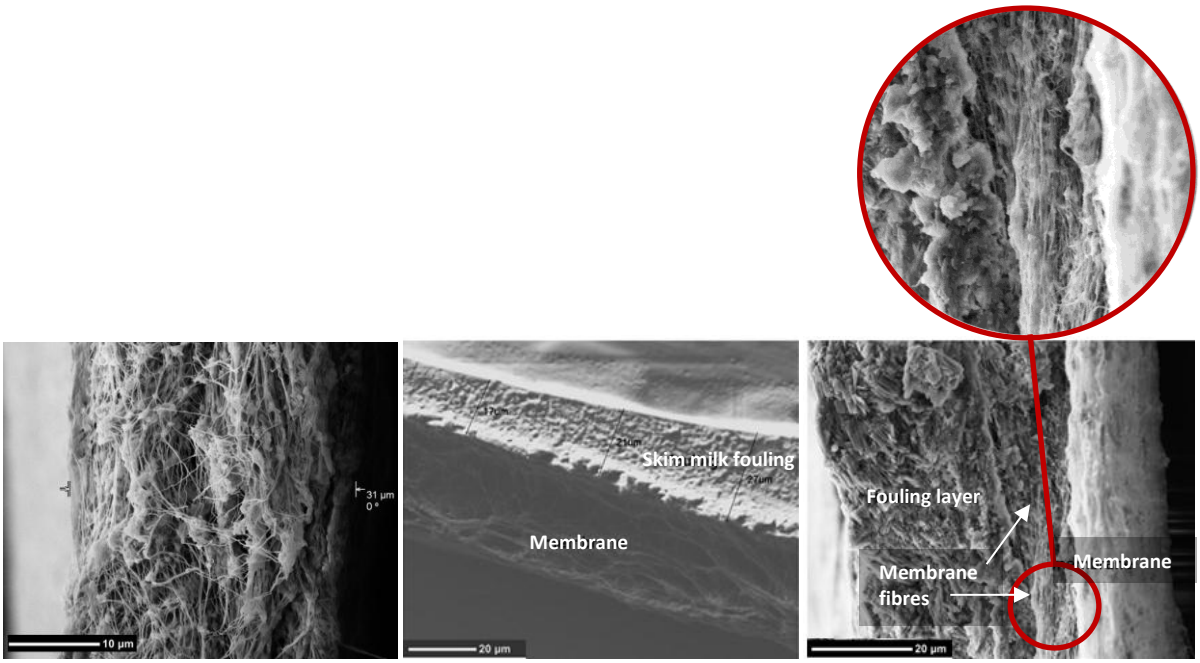

Figure 8: left: unused PTFE membrane (control); middle: skim milk fouled membrane cross-section; right: cross-section of whey fouling layer after 20 hours of operation

The uniform skim milk fouling layer has not obviously penetrated into the membrane structure, whereas some membrane fibres can be detected in the whey fouling layer at its transition point to the membrane. This indicates that the whey fouling layer did not remain on the membrane surface but penetrated at least partly into the web structure of the membrane, therefore reducing its porosity. The thickness of the observed fouling layer was found to be much thinner for skim milk with a fouling layer of around 25 µm, while the whey covered the membrane with an approximately 40 µm thick layer. Despite the thicker whey fouling layer after 18 hours of operation, fluxes of the membranes were similar (results not shown). Whey showed a slower interaction with the surface and although thicker, it may not be as densely packed and can still facilitate water flux to the liquid-vapour interface at the membrane surface. This is confirmed by the mass per cm^2 which results in 0.33 g/cm^3 for skim milk and only 0.13 g/cm^3 for whey.

3.3.2 Elemental scan

Elemental analysis of the cross-section of the membrane and fouling layer gives insight into which components are located close to the membrane surface or even inside the membrane fibre structure and which deposit on top of this initial layer. An elemental scan using SEM-EDS was performed as a surface analysis by focusing on cracks of the fouling layer which occurred as a result of the drying step. This enabled exclusion of any artefact due to sample preparation as compared to a sectioning procedure. As shown in Figure 9 for the skim milk fouling layer, calcium and phosphorus showed very similar distribution towards the membrane sided edge of the crack which could be due to the casein micelles in skim milk containing phosphorus and calcium which work together to form the fouling layer. For the whey fouling layer, on the other hand, calcium was barely present at the membrane but clearly concentrated at the outer edge of the crack within the fouling layer, whereas phosphorus was also present at the membrane sided edge of the crack representing the membrane fouling layer interface. Whey does not contain phospho-proteins contributing to a uniform distribution of these two minerals. The fluorine map relates to the membrane material. The sharper decline in intensity of fluorine for skim milk fouled membranes supports the observation via SEM images that whey anchored inside the membrane web-structure, while skim milk fouling did not anchor as strongly into the membrane pores. The occurrence of minerals inside the membrane structure after MD is in line with findings by Gryta et al. [4] who reported salt deposition inside membranes after DCMD of wastewater.

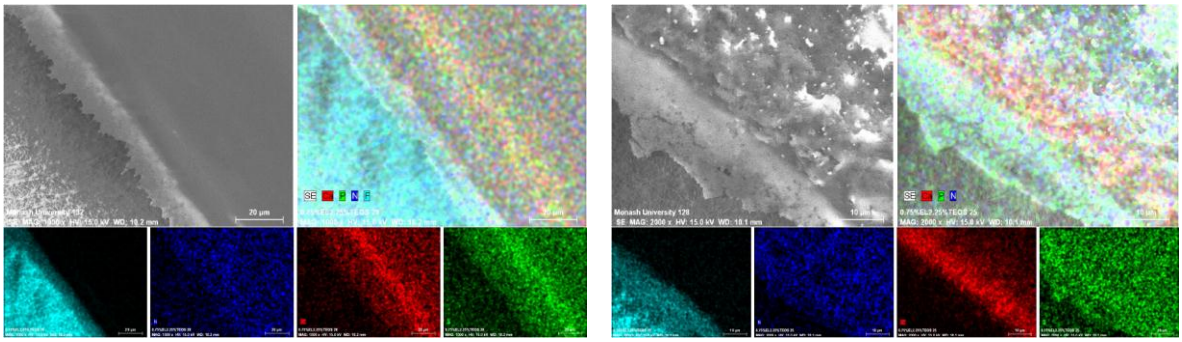

Figure 9: SEM-EDS elemental scan of fouled PTFE membranes after DCMD, left: after skim milk operation, right: after whey operation. Bottom rows show separate distribution of the following elements; from left to right: Fluorine, Nitrogen, Calcium and Phosphorus.

3.3.3 Synchrotron infrared microscopy

Using synchrotron IR spectroscopy, the multilayered nature of the dairy fouling layer can be observed from the perspective of functional groups giving more insight to fouling distribution caused by organic matter. A line scan derived from an area map of the analysed membrane cross-sections is shown in Figure 10. The line of the membrane material (PTFE at 1218 cm^{-1}) shows the location of the membrane on the left side of the graph. Relative length on the x-axis is the length across the membrane to fouling layer cross-section. This measure was used as samples differed in actual thickness. The distribution of peaks at wavenumber 1550 cm^{-1} and 1640 cm^{-1} indicate the distribution of proteinaceous matter [39, 40], confirming that proteins remained on the membrane surface for skim milk, while for whey an overlap with the membrane material occurs. These compounds could be denatured whey proteins interacting with salts or the membrane itself. At wavenumber 1049 cm^{-1} one single peak occurred which is assumed to represent calcium phosphate [41, 42]. This linescan confirms SEM-EDS findings, presented above, where calcium phosphate for the skim milk sample was less involved nearer to the surface. This is also supported by the previous conclusion that caseins in skim milk had a stronger interaction with PTFE on their own, while calcium played a role in accelerating the formation of the fouling layer. Instead, the rise in signal for calcium in the skim milk fouling layer further from the surface in Figure 10 indicates that initial adhesion by proteins can occur when they have a strong interaction with the membrane polymer, while calcium

is involved in bridging proteins to assemble the complete fouling layer. Also, it is worth pointing out that the calcium phosphate signal by IR was stronger in the whey fouling layer supporting the concept that whey proteins form aggregates at the membrane that may have increased ability to bind calcium phosphate due to the exposure of free carboxyl groups [43, 44]. These interactions then result in a protein/calcium phosphate complex. The proximity of calcium to the membrane surface may be a result of whey protein aggregation which requires calcium. These aggregates then migrate into the pores bringing calcium into the pores. Thus in the case of skim milk where less mobile strongly adsorbing proteins were present, they protected the membrane surface from this intrusion from calcium.

Lactose absorbs in a similar range as calcium phosphate, however with a double peak at wavenumbers 1075 and 1042 cm^{-1} [39], a single peak at 1080 cm^{-1} has also been associated with lactose [40]. In the present study a peak at 1080 cm-1 has been detected and is assumed to be related to lactose. As Figure 10 demonstrates, lactose concentration continually increases within the fouling layer which confirms the role of lactose in dairy fouling being related to protein deposition.

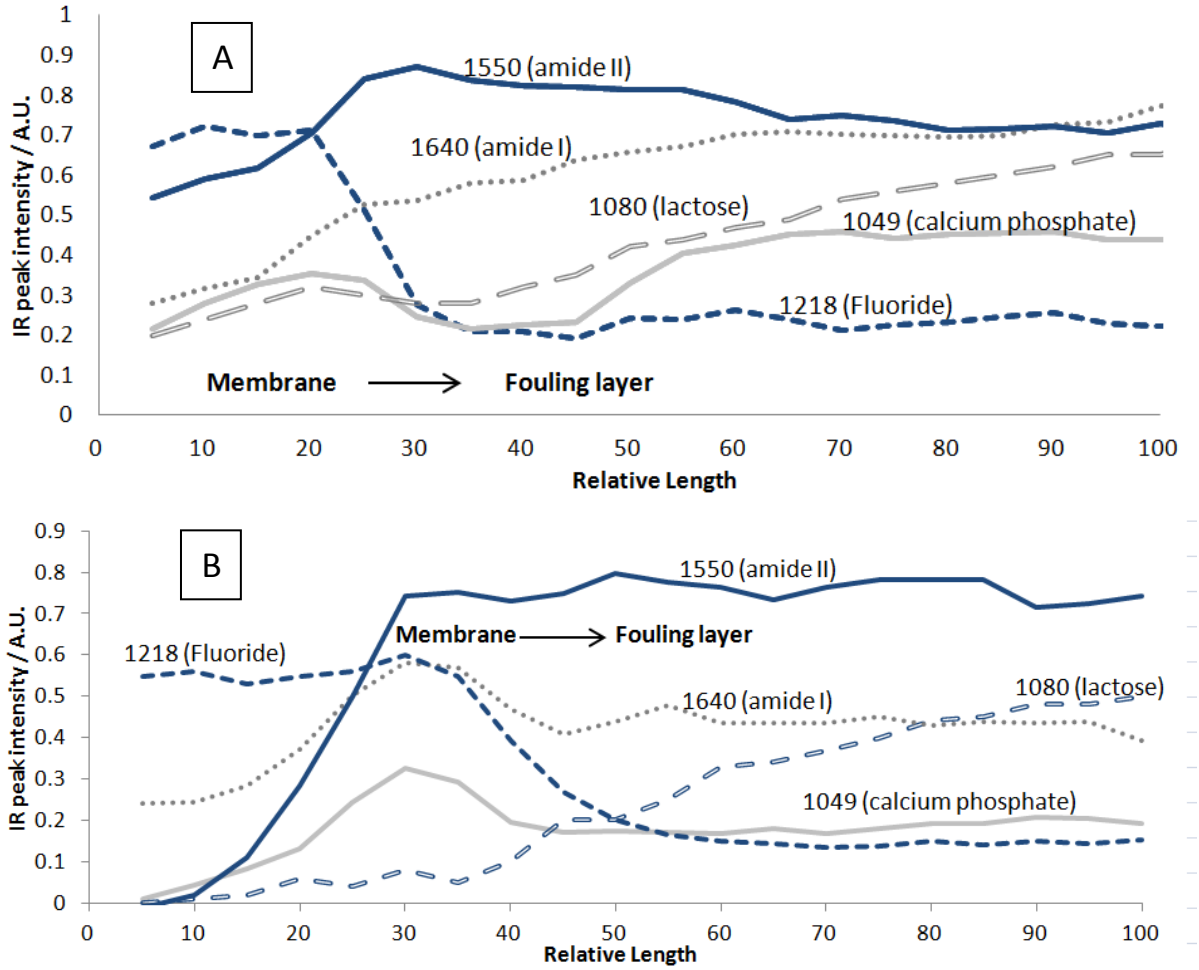

Figure 10: IR line scan along cross-section of membrane and fouling layer, Figure A: skim milk, Figure B: whey; Showing peak intensity of functional groups: 1218 cm^{-1} indicating PTFE, 1081 cm-1 indicating CaP, 1627 and 1461cm^{-1} indicating proteinaceous matter; A.U. = arbitrary units

4.0 Conclusions

Major findings regarding fouling mechanisms for skim milk and whey during membrane distillation include that skim milk fouling started with the deposition of proteins and salts with lactose joining at later fouling stages. In line with this, whey also showed salts and proteins depositing first but then the fouling layer grew more consistently in composition, increasing in total deposition amount of all components in similar relative quantities. Also, whey fouling remained reversible for much longer time periods while skim milk fouling happened within a few minutes. Whey fouling started in patches and grew across the membrane area while skim milk formed a homogeneous layer that grew in thickness. Also, the whey fouling layer was less dense than the skim milk layer which can

explain differences in flux decline as a function of time. Chemistry suggests that caseins adsorb onto the membrane polymer in high amounts and very quickly and compete for area while whey proteins adsorb much slower and need each other to accelerate the adsorption process and to establish a thick layer. During MD of whey, some minerals and proteinaceous material penetrated into the membrane fibres while skim milk caseins seemed to form a protective layer on the membrane surface. This was due to calcium playing a stronger role on adhesion in the presence of whey proteins that interacted slower with the membrane and whey protein aggregation may be an explanation for these interactions. This study has uncovered fouling mechanisms during MD of skim milk and whey and future research to explore ways to reduce protein fouling with these hydrophobic membranes would be of benefit to introduce this process to dairy processing. Furthermore, the influence of operating parameters on fouling mechanisms needs to be explored in order to reduce fouling occurrence.

Acknowledgements

This work was funded by an Australian Research Council Linkage Project (LP0990532) co-funded by Dairy Innovation Australia Ltd. The authors acknowledge the SEM-EDS work by Prof Huanting Wang and Dr Kun Wang at the Department of Chemical Engineering, Monash University. We further acknowledge the Australian Synchrotron for provision of beamtime at the IR beamline and we would like to thank Dr Mark Tobin for his assistance. We also thank Ian Boundy at Hawthorn Histology for preparing the samples suitable for the synchrotron IR work.

References

1. Alkhudhiri, A., N. Darwish, and N. Hilal, Membrane distillation: A comprehensive review. Desalination. 287(0): p. 2-18.

2. Jiao, B., A. Cassano, and E. Drioli, Recent advances on membrane processes for the concentration of fruit juices: a review. Journal of Food Engineering, 2004. 63(3): p. 303-324.

3. Zhang, J., N. Dow, M. Duke, E. Ostarcevic, J.-D. Li, and S. Gray, Identification of material and physical features of membrane distillation membranes for high performance desalination. Journal of Membrane Science, 2010. 349(12): p. 295-303.

4. Gryta, M., Fouling in direct contact membrane distillation process. Journal of Membrane Science, 2008. 325(1): p. 383-394.

5. Chanachai, A., K. Meksup, and R. Jiraratananon, Coating of hydrophobic hollow fiber PVDF membrane with chitosan for protection against wetting and flavor loss in osmotic distillation process. Separation and Purification Technology, 2010. In Press, Corrected Proof.

6. K.K.Sirkar and B. Li, *Novel Membrane and Device for direct contact membrane distillation-based desalination Process: Phase II*. 2003, New Jersey Institute of Technology: Newark, New Jersey.

7. Khayet, M., T. Matsuura, J.I. Mengual, and M. Qtaishat, Design of novel direct contact membrane distillation membranes. Desalination, 2006. 192(1-3): p. 105-111.

8. Piry, A., W. Kühnl, T. Grein, A. Tolkach, S. Ripperger, and U. Kulozik, Length dependency of flux and protein permeation in crossflow microfiltration of skimmed milk. Journal of Membrane Science, 2008. 325(2): p. 887-894.

9. Mourouzidis-Mourouzis, S.A. and A.J. Karabelas, Whey protein fouling of microfiltration ceramic membranes--Pressure effects. Journal of Membrane Science, 2006. 282(1-2): p. 124-132.

10. James, B.J., Y. Jing, and X. Dong Chen, Membrane fouling during filtration of milk--a microstructural study. Journal of Food Engineering, 2003. 60(4): p. 431-437.

11. Grandison, A.S., W. Youravong, and M.J. Lewis, Hydrodynamic factors affecting flux and fouling during ultrafiltration of skimmed milk. Le Lait, 2000. 80: p. 165 - 174.

12. Bouzid, H., M. Rabiller-Baudry, L. Paugam, F. Rousseau, Z. Derriche, and N.E. Bettahar, Impact of zeta potential and size of caseins as precursors of fouling deposit on limiting and critical fluxes in spiral ultrafiltration of modified skim milks. Journal of Membrane Science, 2008. 314(1-2): p. 67-75.

13. Jimenez-Lopez, A.J.E., N. Leconte, F. Garnier-Lambrouin, A. Bouchoux, F. Rousseau, and G. Gésan-Guiziou, Ionic strength dependence of skimmed milk microfiltration: Relations between filtration performance, deposit layer characteristics and colloidal properties of casein micelles. Journal of Membrane Science, 2011. 369(1-2): p. 404-413.

14. Bégoin, L., M. Rabiller-Baudry, B. Chaufer, C. Faille, P. Blanpain-Avet, T. Bénézech, and T. Doneva, Methodology of analysis of a spiral-wound module. Application to PES membrane for ultrafiltration of skimmed milk. Desalination, 2006. 192(1-3): p. 40-53.

15. Sing, H. and P. Havea, *Thermal denaturation, aggregation and gelation of whey proteins*, in *Advanced Dairy Chemistry-Proteins Part A*, P.F. Fox. and P.L.H. Mcsweeney, Editors. 2003, Kluwer Academic, Plenum Publishers: New York. NY p. 1263 - 1281.

16. Zhang, J., J.-D. Li, and S. Gray, Effect of applied pressure on performance of PTFE membrane in DCMD. Journal of Membrane Science, 2011. 369(12): p. 514-525.

17. Chanachai, A., K. Meksup, and R. Jiraratananon, Coating of hydrophobic hollow fiber PVDF membrane with chitosan for protection against wetting and flavor loss in osmotic distillation process. Separation and Purification Technology, 2010. 72(2): p. 217-224.

18. Xu, J.B., S. Lange, J.P. Bartley, and R.A. Johnson, Alginate-coated microporous PTFE membranes for use in the osmotic distillation of oily feeds. Journal of Membrane Science, 2004. 240(1-2): p. 81-89.

19. Ramchandran, L., P. Sanciolo, T. Vasiljevic, M. Broome, I. Powell, and M. Duke, Improving cell yield and lactic acid production of Lactococcus lactis ssp. cremoris by a novel submerged membrane fermentation process. Journal of Membrane Science. 403â€“404(0): p. 179-187.

20. Kira, C.S. and V.A. Maihara, Determination of major and minor elements in dairy products through inductively coupled plasma optical emission spectrometry after wet partial digestion and neutron activation analysis. Food Chemistry, 2007. 100(1): p. 390-395.

21. van der Ven, C., S. Muresan, H. Gruppen, D.B.A. de Bont, K.B. Merck, and A.G.J. Voragen, FTIR Spectra of Whey and Casein Hydrolysates in Relation to Their Functional Properties. Journal of Agricultural and Food Chemistry, 2002. 50(24): p. 6943-6950.

22. Metsämuuronen, S., M. Mänttäri, and M. Nyström, Comparison of analysis methods for protein concentration and its use in UF fractionation of whey. Desalination. In Press, Corrected Proof.

23. Ferlita, R.R., D. Phipps, J. Safarik, and D.H. Yeh, Cryo-snap: A simple modified freeze-fracture method for SEM imaging of membrane cross-sections. Environmental Progress, 2008. 27(2): p. 204-209.

24. Schroen, C.G.P.H., A. Roosjen, K. Tang, W. Norde, and R.M. Boom, In situ quantification of membrane foulant accumulation by reflectometry. Journal of Membrane Science. 362(12): p. 453-459.

25. Nady, N., K. Schroën, M.C.R. Franssen, R. Fokkink, M.S. Mohy Eldin, H. Zuilhof, and R.M. Boom, Enzyme-catalyzed modification of PES surfaces: Reduction in adsorption of BSA, dextrin and tannin. Journal of Colloid and Interface Science. 378(1): p. 191-200.

26. Dijt, J.C., M.A.C. Stuart, J.E. Hofman, and G.J. Fleer, Kinetics of polymer adsorption in stagnation point flow. Colloids and Surfaces, 1990. 51(0): p. 141-158.

27. Dijt, J.C., M.A.C. Stuart, and G.J. Fleer, Reflectometry as a tool for adsorption studies. Advances in Colloid and Interface Science, 1994. 50(0): p. 79-101.

28. McSweeney, P.L.H. and P.F. Fox, *Advanced Dairy Chemistry: Volume 3: Lactose, Water, Salts and Minor Constituents*. 2009: Springer Science and Business Media.

29. Goulden, J.D.S., Determination of S.N.F. in milk and unsweetened condensed milk from refractive index measurements. Journal of Dairy Research, 1963. 30(03): p. 411-417.

30. Chaudhuri, R.G. and S. Paria, Dynamic contact angles on PTFE surface by aqueous surfactant solution in the absence and presence of electrolytes. Journal of Colloid and Interface Science, 2009. 337(2): p. 555-562.

31. Fox, P.F. and P.L.H. McSweeney, *Dairy Chemistry and Biochemistry*. 1998, London: Blackie Academic & Professional.

32. Jucker, B.A., H. Harms, and A.J. Zehnder, Adhesion of the positively charged bacterium Stenotrophomonas (Xanthomonas) maltophilia 70401 to glass and Teflon. J Bacteriol., 1996. 178(18): p. 5472–5479.

33. de la Fuente, M.A., H. Singh, and Y. Hemar, Recent advances in the characterisation of heat-induced aggregates and intermediates of whey proteins. Trends in Food Science & Technology, 2002. 13(8): p. 262-274.

34. Bottino, A., G. Capannelli, O. Monticelli, and P. Piaggio, Poly(vinylidene fluoride) with improved functionalization for membrane production. Journal of Membrane Science, 2000. 166(1): p. 23-29.

35. Howe, K.J. and M.M. Clark, Fouling of Microfiltration and Ultrafiltration Membranes by Natural Waters. Environmental Science & Technology, 2002. 36(16): p. 3571-3576.

36. Liu, C., S. Caothien, J. Hayes, T. Caothuy, and T. Otoyo. *Membrane chemical cleaning: from art to science*. 2008 12.2.2009]; Available from: http://www.pall.com/pdf/mtcpaper.pdf.

37. Creamer, L.K., J.E. Plowman, M.J. Liddell, M.H. Smith, and J.P. Hill, Micelle Stability: kappa-Casein Structure and Function. Journal of Dairy Science, 1998. 81(11): p. 3004-3012.

38. Glover, F.A., *Ultrafiltration and reverse osmosis for the dairy industry*. Vol. Technical Bulletin 5. 1985, Reading: National Institute for Research in Dairying.

39. Myrna Solís-Oba, Ogilver Teniza-García, Marlon Rojas-López, Raúl Delgado-Macuil, Joel Díaz-Reyes, and R. Ruiz1, Application of Infrared Spectroscopy to the Monitoring of Lactose and Protein From Whey After Ultra and Nano Filtration Process. Journal of the Mexican Chemical Society, 2011. 55(3): p. 190-193.

40. Grenvall, C., P. Augustsson, J.R. Folkenberg, and T. Laurell, Harmonic Microchip Acoustophoresis: A Route to Online Raw Milk Sample Precondition in Protein and Lipid Content Quality Control. Analytical Chemistry, 2009. 81(15): p. 6195-6200.

41. Anema, S., G., Stability of milk-derived calcium phosphate suspensions. Dairy Sci. Technol., 2009. 89(3-4): p. 269-282.

42. Ślósarczyk, A., C.a. Paluszkiewicz, M. Gawlicki, and Z. Paszkiewicz, The FTIR spectroscopy and QXRD studies of calcium phosphate based materials produced from the powder precursors with different CaP ratios. Ceramics International, 1997. 23(4): p. 297-304.

43. O'Kennedy, B.T., C. Halbert, and P.M. Kelly, Formation of whey protein particles using calcium phosphate and their subsequent stability to heat. Milchwissenschaft, 2001. 56(11): p. 625-628.

44. Halbert, C., B.T. O'Kennedy, A. Hallihan, and P.M. Kelly, Stabilisation of calcium phosphate using denatured whey proteins. Milchwissenschaft, 2000. 55(7): p. 386-389.